Hindawi Publishing Corporation
Journal of Nanomaterials
Volume 2013, Article ID 954621, 8 pages
http://dx.doi.org/10.1155/2013/954621

Research Article

Magnetic Properties and Microstructure of FeO_x/Fe/FePt and FeO_x/FePt Films

Jai-Lin Tsai, Po-Ran Chen, Yi-Hsiu Chen, and Qi-Shao Luo

Department of Materials Science and Engineering, National Chung Hsing University, 250 Kuo Kuang Road, Taichung 402, Taiwan

Correspondence should be addressed to Jai-Lin Tsai; tsaijl@dragon.nchu.edu.tw

Received 9 July 2013; Revised 13 August 2013; Accepted 15 August 2013

Academic Editor: Guangyu Zhao

The Fe(6 nm)/FePt film with perpendicular magnetization was deposited on the glass substrate. To study the oxygen diffusion effect on the coupling of Fe/FePt bilayer, the plasma oxidation with 0.5~7% oxygen flow ratio was performed during sputtered part of Fe layer and formed the FeO_x(3 nm)/Fe(3 nm)/FePt trilayer. Two-step magnetic hysteresis loops were found in trilayer with oxygen flow ratio above 1%. The magnetization in FeO_x and Fe/FePt layers was decoupled. The moments in FeO_x layer were first reversed and followed by coupled Fe/FePt bilayer. The trilayer was annealed again at 500°C and 800°C for 3 minutes. When the FeO_x(3 nm)/Fe(3 nm)/FePt trilayer was annealed at 500°C, the layers structure was changed to FeO_x(6 nm)/FePt bilayer due to oxygen diffusion. The hard-magnetic FeO_x(6 nm)/FePt film was coupled with single switching field. The FeO_x/(disordered FePt) layer structure was observed with further annealing at 800°C and presented soft-magnetic loop. In summary, the coupling between soft-magnetic Fe, FeO_x layer, and hard-magnetic $L1_0$ FePt layer can be controlled by the oxygen diffusion behavior, and the oxidation of Fe layer was tuned by the annealing temperature. The ordered $L1_0$ FePt layer was deteriorated by oxygen and became disordered FePt when the annealed temperature was up to 800°C.

1. Introduction

Equiatomic FePt film with anisotropic face-centered tetragonal (fct) $L1_0$ ordered structure has high magnetocrystalline anisotropy which is the promised material in energy assisted perpendicular magnetic recording. The $L1_0$ FePt phase was ordered from disordered FePt phase with face-centered cubic (fcc) structure after high temperature annealing [1–6]. The disordered and $L1_0$ FePt phases show soft- and hard-magnetic properties, respectively. The ordering degree can be changed from 0 (disordered) to 1 (ordered) that depends on the process temperature or condition. The granular structure with columnar grains [7, 8] and well *c*-axis alignment normal to the film surface with low switching field distribution are required for FePt perpendicular recording media. For *c*-axis alignment, [001] textured FePt films have been prepared on amorphous glass substrate or MgO underlayer with lower ordering temperatures [9–11]. To write in perpendicular recording media, measure can be taken from energy assisted writing process called heat assisted magnetic recording (HAMR) [12]. To down the writing temperature under fixed writing field, minor adjusting of the intrinsic magnetic anisotropy of FePt film was required. The magnetic anisotropy and the coercivity of FePt film can be tuned by composition and the third element addition [13]. The [001] textured FePt film was not easily formed when target composition far deviated from equal atomic ration. In addition, the magnetic anisotropy was usually diluted by nonmagnetic doping. As a result, it is necessary to have high [001] textured FePt granular film with lower coercivity that was accepted by writing temperature and field. Traditionally, exchange spring media and exchange coupled composite (ECC) media with higher and lower magnetic anisotropic layer were introduced to reduce the writing field requirement and maintain the same thermal stability and grater insensitivity to easy axis [14–20]. The motivations of this work are try (1) to know the oxygen diffusion effects on magnetic properties of FePt film and prove the change of magnetic properties by the second annealing process, (2) to modify the morphology of dewetted FePt film by FeO_x, and (3) to study the coupling effect via FeO_x/Fe/FePt trilayer structure. The structure of FeO_x may be cubic FeO, tetragonal γ-Fe_2O_3 (maghemite)

or spinel Fe_3O_4 (magnetite), with ferrimagnetism. Plasma oxidation and further annealing were proposed and proven to change the magnetic properties and microstructure of FeO_x/Fe/FePt films. The [001] textured FeO_x/FePt dewetted film with perpendicular magnetization was also observed.

2. Experimental

The FePt film was deposited on a glass substrate at room temperature (RT) by magnetron sputtering. The sputtering system was designed for ultrahigh vacuum with base pressure of 5×10^{-8} Torr, and the load-lock system was used to transfer the substrate via prechamber with base pressure of 5×10^{-7} Torr. The FePt and Fe targets were used, and a working pressure was fixed at 1.5×10^{-3} Torr under high purity argon gas. The total thickness of FePt film is 10 nm, and the chemical composition of the FePt layer was $Fe_{48}Pt_{52}$ measured by an energy dispersive spectrometer (EDS) on a single thicker FePt layer. After deposition, the films were annealed under argon atmosphere by using a rapid thermal annealing process (RTP) at 800°C for 3 minutes with heating rate of 10°C/s and formed the $L1_0$ FePt thin film. The Fe layer with thickness of 6 nm was deposited at RT on FePt film and formed the Fe/FePt bilayer. To study the oxygen diffusion effect on the coupling of Fe(6 nm)/FePt bilayer, the plasma oxidation with varied oxygen flow ration [$P = P_{O_2}/(P_{O_2} + P_{Ar}) = 0.3, 0.5, 1, 3, 7\%$] was performed during sputtered part of Fe layer and formed the FeO_x(3 nm)/Fe(3 nm)/FePt trilayer. More precisely, the oxygen was introduced during sputtering in half of the Fe layer thickness which is 3 nm. The trilayer was further annealed at 500°C, 800°C and finally formed the FeO_x/FePt, FeO_x/(disordered FePt), respectively. The thickness of each layer or sputtering rate of each material was measured by atomic force microscopy. The crystal structure of the samples was identified using a standard X-ray diffraction (XRD) technique (BRUKER, D8 Discover). The film microstructure was observed by scanning electron microscopy (JEOL JSM-6700F) and atomic force microscopy (DI 3100). The surface chemical property was measured by X-ray photoelectron spectroscopy ((XPS) PHI5000VersaProbe). Magnetic hysteresis loops were measured at room temperature using a vibration sample magnetometer ((VSM) Lakeshore 7400) with a maximum magnetic field of 2T. The magnetic field was applied to be parallel and perpendicular to film surface to obtain in-plane and out-of-plane hysteresis loops, respectively.

3. Results and Discussion

Figures 1(a)–1(f) show standard XRD patterns of FePt single layer, Fe(6 nm)/FePt bilayer, and FeO_x/Fe/FePt films. In Figure 1(a), the FePt single layer was ordered in $L1_0$ phase, and the (001) superlattice diffraction peak and the (002) fundamental reflection are clearly observed. The XRD profiles suggest that the $L1_0$ FePt crystal has a [001] texture. Figures 1(b)–1(f) show the XRD patterns of Fe(6 nm)/FePt bilayer and FeO_x(P)/Fe/FePt trilayer (P = 0.5, 1, 3, and 7%). In Figures 1(b)–1(f), the $L1_0$ FePt films also show strong (001) and (002)

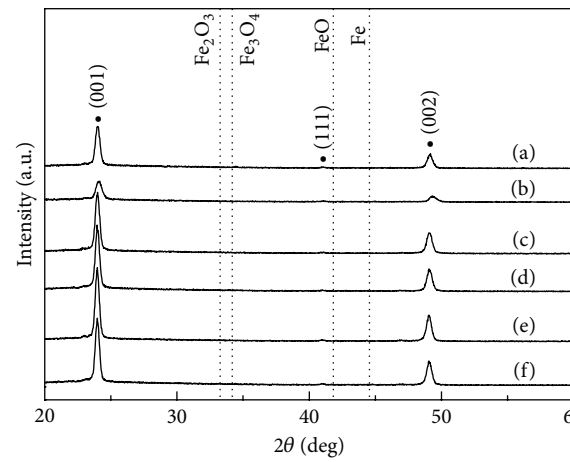

Figure 1: XRD patterns of (a) FePt single layer, (b) Fe(6 nm)/FePt bilayer, and FeO_x(P)/Fe/FePt films with different oxygen flow rationes, P = (c) 0.5%, (d) 1%, (e) 3%, and (f) 7%.

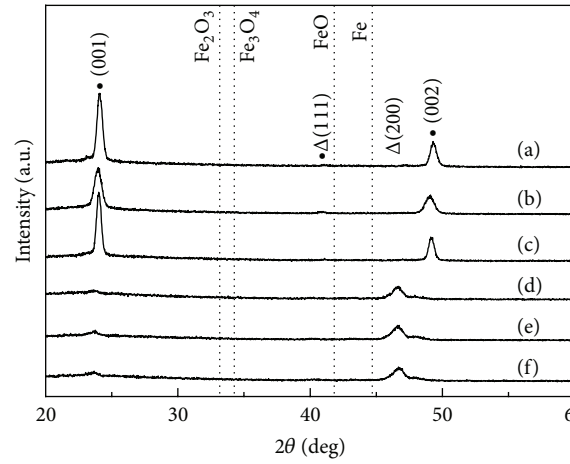

Figure 2: XRD patterns of FeO_x(P)/Fe/FePt trilayer further annealed at 500°C with P = (a) 1%, (b) 3%, and (c) 7% and 800°C with P = (d) 1%, (e) 3%, (f) 7%.

peaks that were not smeared out by Fe and FeO_x deposited at RT. The peaks of Fe and FeO_x were not found in standard X-ray diffraction (XRD) due to strong FePt (001) texturing. The standard X-ray peaks of Fe (JCPDS 89-7194), FeO (JCPDS 89-7100), Fe_2O_3 (JCPDS 89-8104), and Fe_3O_4 (JCPDS 89-6466) were marked in Figures 1 and 2. The ordering parameter, S, was calculated from $(I^*_{(002)}/I^*_{(001)})^{1/2}$ $(I_{(001)}/I_{(002)})^{1/2}$ or proportional to $I_{(001)}/I_{(002)}$ ratio [21]. The $(I^*_{(002)}/I^*_{(001)})^{1/2}$ value, for example, 0.4915 in $L1_0$ FePt film, was obtained after considering all the corrected factors in the XRD data. Fully-ordered $L1_0$ FePt X-ray diffraction peak intensity is given by $(I^*_{002}/I^*_{001}) = (|F|^2 \times \mathrm{LPDA})_{002}/(|F|^2 \times \mathrm{LPDA})_{001}$ [21]. For $L1_0$ FePt, the structure factor F is $F_{hkl} = f_{Fe}(1 + e^{\pi i(h+k)}) + f_{Pt}(e^{\pi i(k+l)} + e^{\pi i(h+l)})$, and f is atomic scattering factor [21]. The

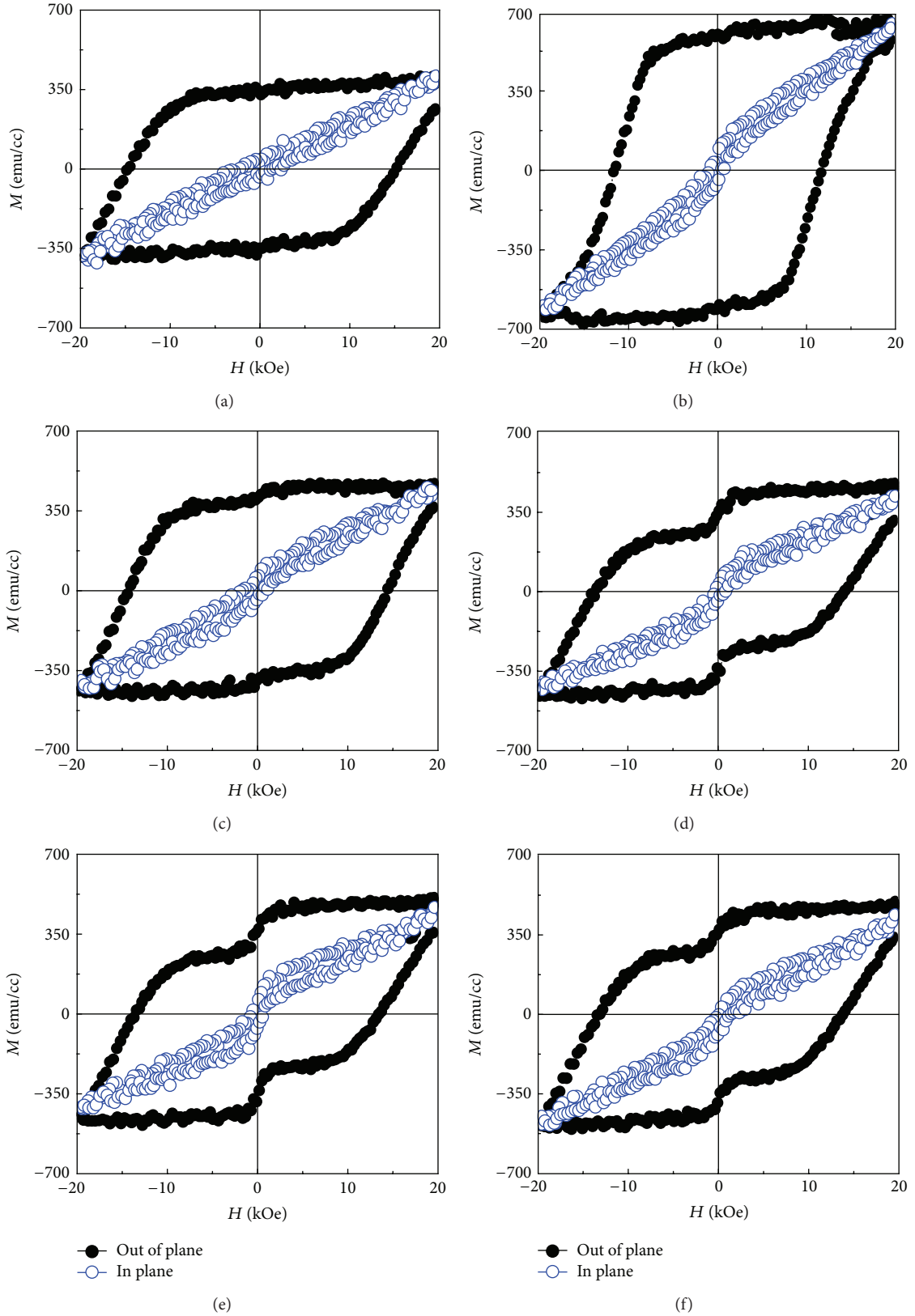

FIGURE 3: In-plane and out-of-plane magnetic hysteresis loops of (a) FePt single layer, (b) Fe(6 nm)/FePt bilayer, and FeO_x(P)/Fe/FePt films with different oxygen flow rationes; P = (c) 0.5%, (d) 1%, (e) 3%, and (f) 7%.

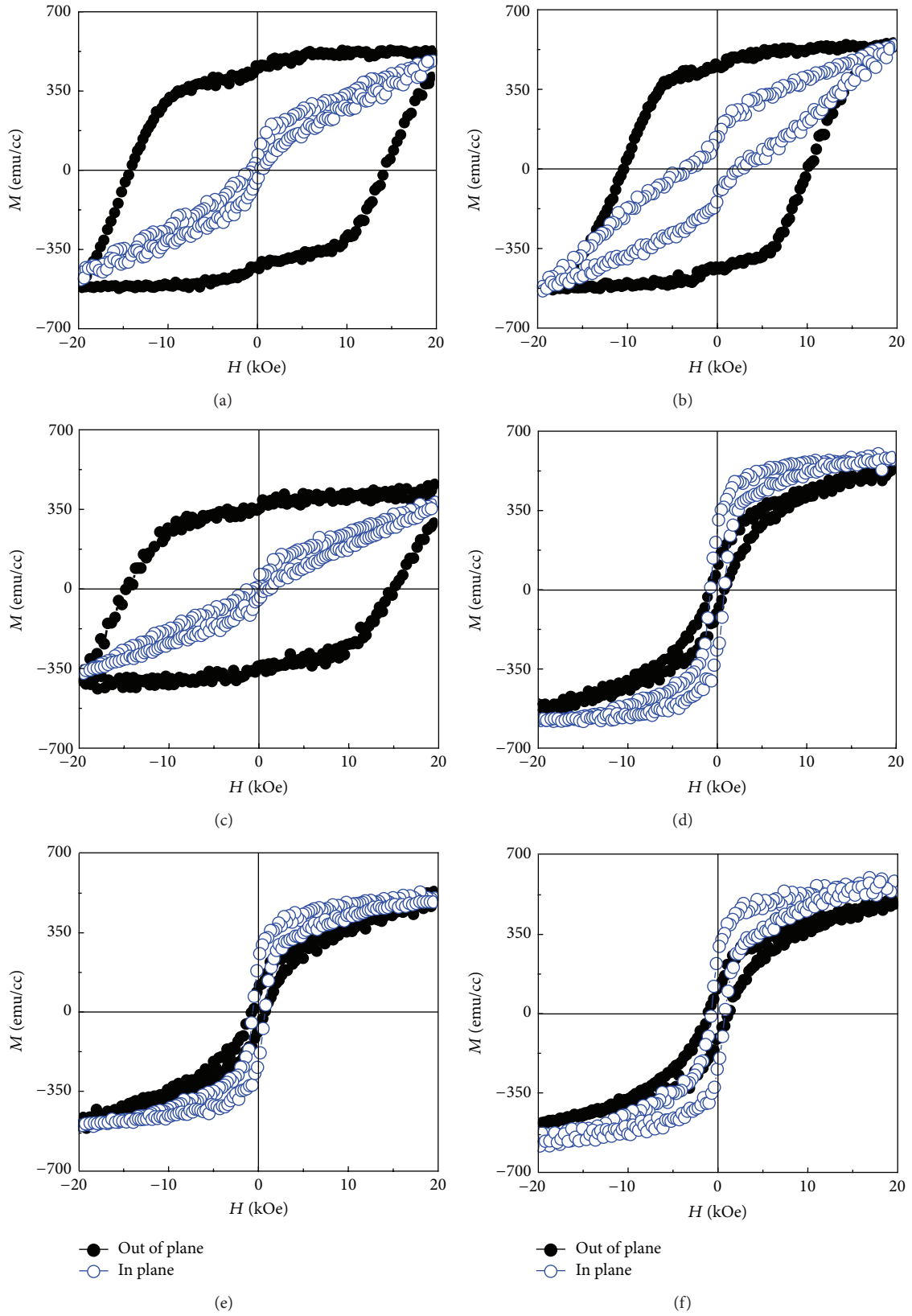

FIGURE 4: In-plane and out-of-plane magnetic hysteresis loops of FeO_x(P)/Fe/FePt trilayer further annealed at 500°C with P = (a) 1%, (b) 3%, and (c) 7% and 800°C with P = (d) 1%, (e) 3%, and (f) 7%.

Lorentz factor (L) is $[1/\sin^2(\theta)\cos(\theta)]$, and the polarization factor (P) is $(1 + \cos^2(2\theta))$. The temperature factor (D) is e^{-2M} and $M = (\sin(\theta)/\lambda)^2$, and absorption factor (A) is $1 - \exp(-2\mu t/(\sin\theta))$. The average mass absorption coefficient was estimated as $\mu = [\mu_{Fe} \times \text{wt\%Fe} + \mu_{Pt} \times \text{wt\%Pt}] \times [X_{Fe}\rho_{Fe} + X_{Pt}\rho_{Pt}]$ [21], and the value is 3323.8 in this study. Here, X_{Fe}, X_{Pt} and ρ_{Fe}, ρ_{Pt} are the atomic fraction and density of Fe and Pt, respectively. The values for μ_{Fe} and μ_{Pt} are tabulated [21]. $I^*_{(001)}$ and $I^*_{(002)}$ mean the theoretical integrated intensity of X-ray diffraction peaks, and the $I_{(001)}$ and $I_{(002)}$ are the integrated peak intensity from the experimental results for a partially ordered film. In Figure 1(a), the ordering parameter S estimated from $(I^*_{(002)}/I^*_{(001)})^{1/2}(I_{(001)}/I_{(002)})^{1/2}$ is 0.75, and the S value in Figures 1(c)–1(f) is 0.71~0.72.

Figures 2(a)–2(f) show standard XRD patterns of FeO_x/Fe/FePt trilayer further annealed at 500°C and 800°C, respectively. In Figures 2(a)–2(c), the FeO_x/Fe/FePt trilayer was further annealed at 500°C and became FeO_x/FePt bilayer. In addition to the wideness (full width of half maximum (FWHM)) of (001) and (002) peaks in Figure 2(b), the $L1_0$ FePt still shows strong (001) texture. It means that the $L1_0$ FePt layer was not influenced almost by further being annealed at 500°C. In Figures 2(d)–2(f), the FeO_x/Fe/FePt trilayer was further annealed at 800°C, and the (001) texture was almost diminished, and (200) disordered FePt peak was observed. It is suggested that the oxygen was diffused into the $L1_0$ FePt layer and the layer, structure was changed to FeO_x/(disordered FePt). The FePt (111) peak was not found in standard XRD patterns in Figures 1 and 2 due to strong FePt (001) texture. The ordered or disordered FePt (111) peak was indexed in grazing incident X-ray diffraction (GID). The nonsymmetric GID was used to measure the grains in nonoriented area in textured film.

Figure 3 shows in-plane and out-of-plane magnetic hysteresis loops of FePt single layer, Fe(6 nm)/FePt bilayer, and FeO_x(3 nm)/Fe(3 nm)/FePt trilayer. In Figure 3(a), the FePt single layer shows high perpendicular magnetization, and the out-of-plane coercivity (H_c) is 15.3 kOe. The component in in-plane magnetization is nearly zero and shows the linear loop. In Figure 3(b), the magnetization was increased, and the H_c was reduced to 11.8 kOe in soft/hard exchange coupled Fe/FePt bilayer. Figures 3(c)–3(f) show the loops of FeO_x/Fe/FePt trilayer with different oxygen flow rationes $[P = P_{O_2}/(P_{O_2} + P_{Ar}) = 0.5, 1, 3, 7\%]$. In Figure 3(c), there is just a minor shoulder in the loop of FeO_x/Fe/FePt film with low oxygen flow rationes ($P = 0.5\%$). When the oxygen flow ration was increased to 1, 3, and 7%, the step or shoulder was found in magnetization curve in Figures 3(d)–3(f). The FeO_x layer was decoupled to the Fe/FePt bilayer and reversed the magnetization previously. The magnetization in FeO_x layer was decreased as the negative applied field increased, and, up to the critical value, the magnetization was not changed with increased field. The critical value was defined as the H_c of FeO_x layer. In Figures 3(d)–3(f), the H_c of the FeO_x layer is 1.37, 1.66, and 1.09 kOe, and the H_c values of Fe(3 nm)/FePt bilayer are 13.7, 13.7, and 13.4 kOe, respectively. The H_c value of Fe(3 nm)/FePt is between FePt single layer in Figure 3(a) and Fe(6 nm)/FePt in Figure 3(b).

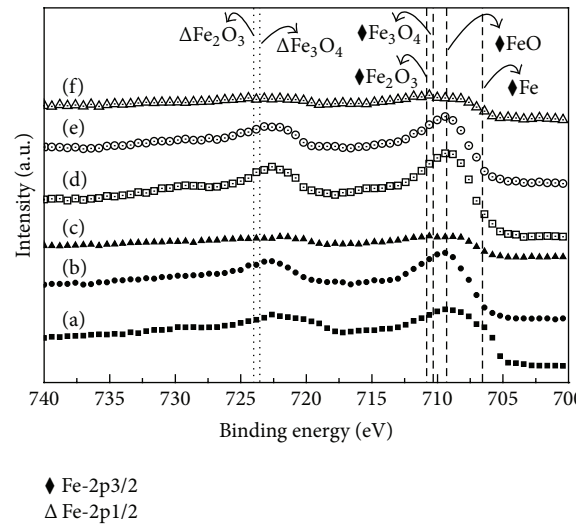

Figure 5: The Fe-2p X-ray photoelectron spectra of FeO_x(3 nm)/Fe(3 nm)/FePt films at the depth position below 3 nm from film surface: (a) RT, (b) 500°C, and (c) 800°C, and at the depth position within 3 nm from film surface: (d) RT, (e) 500°C, and (f) 800°C.

The samples in Figures 3(d)–3(f) are the same to Figures 4(a)–4(c). The trilayers (samples in Figures 3(d)–3(f)) were further annealed at 500°C and 800°C, respectively. Figure 4 shows in-plane and out-of-plane magnetic hysteresis loops of annealed FeO_x(3 nm)/Fe(3 nm)/FePt trilayer. Figures 4(a)–4(c) show the loops of FeO_x(3 nm)/Fe(3 nm)/FePt films annealed at 500°C with oxygen flow ration of 1%, 3%, and 7%, respectively The shoulders appearing in the loops in Figures 3(d)–3(f) disappeared after further annealing. and the loops present single magnetization reversal process. It suggested that the Fe layer was further oxidative, and the layer structure was changed to exchange coupled FeO_x/FePt film. In Figures 4(a)–4(c), the out-of-plane H_c were 14.4, 10.4, and 14.8 kOe which are similar to the measured H_c in Figures 3(d)–3(f). Figures 4(d)–4(f) show the loops of FeO_x(3 nm)/Fe(3 nm)/FePt films annealed at 800°C with oxygen flow ration of 1%, 3%, and 7%, respectively, and the soft-magnetic loops were obtained. The oxygen was diffused into FePt layer and disordered the $L1_0$ phase, and the layer structure was changed to FeO_x/(disordered FePt). In summary, the interlayer coupling and magnetic ansiotropy were tuned by the kinetic diffusion behavior of oxygen driven by temperature.

To understand the oxidation state of Fe and FeO_x (oxygen flow ration of 3%) layer in FeO_x(3 nm)/Fe(3 nm)/FePt film, XPS were performed on samples with different depth profiles. Figures 5(a)–5(c) show the Fe-2p X-ray photoelectron spectra of FeO_x(3 nm)/Fe(3 nm)/FePt films at the depth position below 3 nm from film surface. The curve in Figure 5(a) shows the Fe^0 spectrum that is obtained in FeO_x(3 nm)/Fe(3 nm)/FePt film without further annealing. The metallic Fe-$2p^{3/2}$ shows the peak at the binding energy of 706.5 eV [22]. In Figure 5(b), the FeO_x(3 nm)/Fe(3 nm)/FePt films were further annealed at 500°C, and the binding energy shifts the Fe-$2p_{3/2}$ core level to 709~711 eV. This shift may

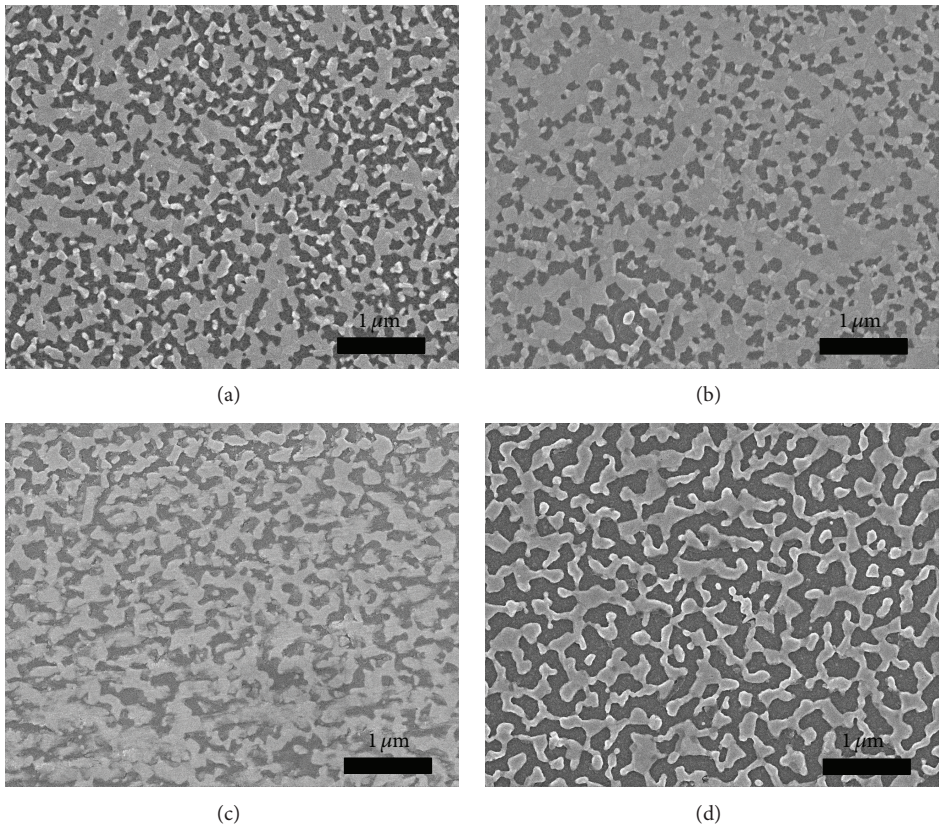

Figure 6: SEM images of (a) Fe/FePt film, (b) FeO_x(7%)/Fe/FePt trilayer, (c) FeO_x(7%)/Fe/FePt film annealed at 500°C, and (d) FeO_x(7%)/Fe/FePt film annealed at 800°C.

prove the formation of iron in the Fe^{2+} oxidation state that was FeO, and the binding energy of the Fe-$2p_{3/2}$ core level was shifted around to 709.6 eV [23]. In Figure 5(c), the FeO_x(3 nm)/Fe(3 nm)/FePt films were further annealed at 800°C, and the peak was smeared out in the iron-oxide area. Figures 5(d)–5(f) show the Fe-2p X-ray photoelectron spectra of FeO_x(3 nm)/Fe(3 nm)/FePt films at the depth within 3 nm from film surface. In Figures 5(d)–5(e), the FeO_x layer before and after further annealing at 500°C was in the Fe^{2+} oxidation state that was FeO, and the binding energy of the Fe-$2p_{3/2}$ core level was shifted around to 709.3 eV. In Figure 5(f), the peak was also smeared out in the iron-oxide area when annealed at 800°C. In summary, first, further annealed at 500°C, the Fe (3 nm) may oxidize or mix with FePt film and form FeO_x/FePt layer structure. Second, further annealed at 800°C, the oxygen was diffused into the FePt lattice, deteriorated the ordering degree, and formed the FeO_x/(disorder FePt) film.

Figure 6 shows the scanning electron microscopy (SEM) image of Fe(6 nm)/FePt and FeO_x(3 nm)/Fe(3 nm)/FePt films with oxygen flow ration of 7%. In Figure 6(a), the annealed Fe(6 nm)/FePt film was dewetted in the network structure, and the dewetted area was 44%. When the Fe layer was partially plasma oxidized and formed the FeO_x(3 nm)/Fe(3 nm)/FePt layer structure, the dewetted area was reduced to 30% as shown in Figure 6(b). The FeO_x has lower surface energy than FePt and was easy to wet on the glass substrate. As a result, the dewetted area was reduced around 14%. In Figures 6(c) and 6(d), the FeO_x(3 nm)/Fe(3 nm)/FePt film was furthered annealed at 500°C, 800°C, and the dewetted area was 42%, 55%, respectively. Due to large difference of surface energy between FePt and glass substrate, the dewetted area was increased again with annealing temperature.

Figure 7 shows the surface roughness of Fe/FePt and FeO_x/Fe/FePt film with oxygen flow ration of 7% measured by atomic force microscopy (AFM). In Figure 7(a), the average surface roughness of Fe/FePt film was 7.1 nm. In Figures 7(b) and 7(c), when the FeO_x layer was capped on Fe/FePt film at RT without annealing or with further annealing at 500°C, the average surface roughness became 4.9 nm and 3.2 nm, respectively. In Figure 7(d), the surface roughness was up to 13 nm when the annealed temperature was high to 800°C. In summary, the dewetted area in Fe/FePt film was partially covered by FeO_x layer deposited at RT but aggregated into small area again with further annealing at high temperature. The surface roughness shows the same tendency to the dewetted area. The FePt film with thickness of 10 nm was dewetted due to strain release when the ordering (rapid phase transformation) was complete at 800°C. The dewetted area and surface roughness were increased with annealing temperature, and the critical dewetted temperature is 650°C in this study. After annealing, the sample was cooled down naturally in the argon atmosphere in RTP system. Cooling rate was not changed in this experiment and will be check in the future.

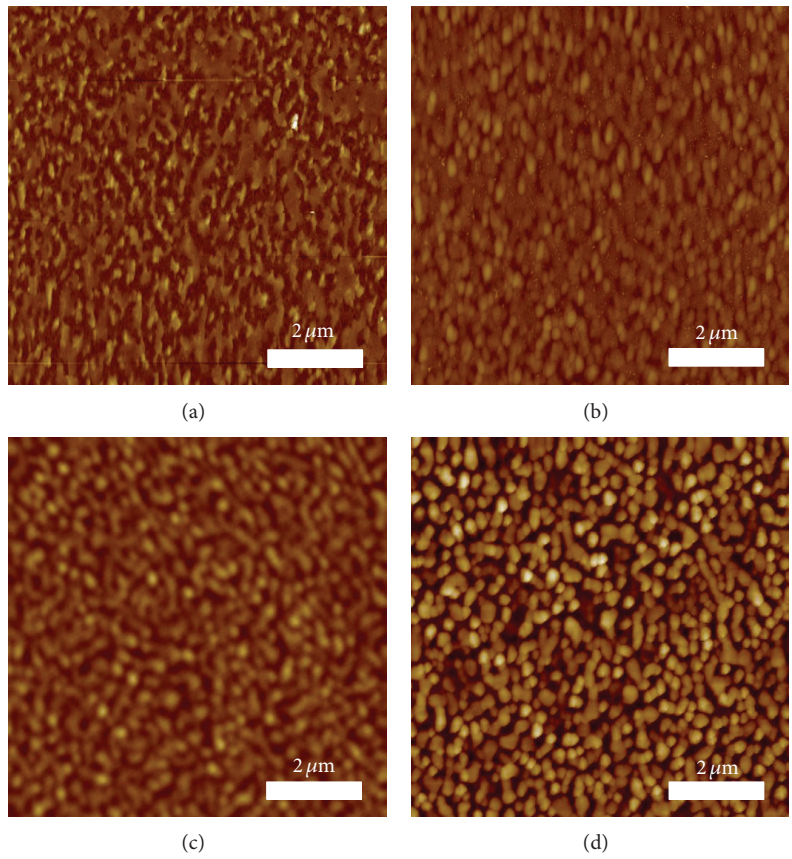

FIGURE 7: AFM images of (a) Fe/FePt film, (b) FeO_x(7%)/Fe/FePt trilayer, (c) FeO_x(7%)/Fe/FePt film annealed at 500°C, and (d) FeO_x(7%)/Fe/FePt film annealed at 800°C.

4. Conclusions

The plasma oxidation was performed during sputtered part of Fe layer in Fe/FePt film and formed the FeO_x(3 nm)/Fe(3 nm)/FePt trilayer. The magnetization in FeO_x and Fe/FePt layers was decoupled and shown the shoulders in hysteresis loops. When the FeO_x(3 nm)/Fe(3 nm)/FePt trilayer was further annealed at 500°C, the layers structure was changed to FeO_x(6 nm)/FePt bilayer due to oxygen diffusion. The hard-magnetic FeO_x(6 nm)/FePt film was coupled with single switching field. The coupling between soft-magnetic Fe, FeO_x layer, and hard-magnetic $L1_0$ FePt layer was tuned by two-stage annealing process.

Acknowledgments

The authors would like to thank the National Science Council, Taiwan, for financial support under the Grant no. NSC 102-2221-E-005-025. They also thank the Center of Nanoscience and Nanotechnology in NCHU for TEM investigations.

References

[1] D. Weller, A. Moser, L. Folks et al., "High ku materials approach to 100 gbits/in2," *IEEE Transactions on Magnetics*, vol. 36, no. 1, pp. 10–15, 2000.

[2] M. H. Hong, K. Hono, and M. Watanabe, "Microsturcture of FePt/Pt magnetic thin films with high perpendicular coercivity," *Journal of Applied Physics*, vol. 84, pp. 4403–4409, 1998.

[3] S. N. Piramanayagam, "Perpendicular recording media for hard disk drives," *Journal of Applied Physics*, vol. 102, no. 1, Article ID 011301, 22 pages, 2007.

[4] H. J. Richter, "The transition from longitudinal to perpendicular recording," *Journal of Physics D*, vol. 40, no. 9, article R149, 2007.

[5] J. P. Liu, C. P. Luo, Y. Liu, and D. J. Sellmyer, "High energy products in rapidly annealed nanoscale Fe/Pt multilayers," *Applied Physics Letters*, vol. 72, no. 4, article 483, 3 pages, 1998.

[6] T. Shima, K. Takanashi, Y. K. Takahashi, and K. Hono, "Formation of octahedral FePt nanoparticles by alternate deposition of FePt and MgO," *Applied Physics Letters*, vol. 88, no. 6, Article ID 063117, 3 pages, 2006.

[7] H. H. Li, J. F. Hu, G. Ju, G. M. Chow, and J. S. Chen, "Effects of CrRu-SiOx underlayer with MgO intermediate layer on the microstructure and magnetic properties of FePt-C film," *Journal of Applied Physics*, vol. 109, Article ID 07A736, 2009.

[8] E. Yang, H. Ho, D. E. Laughlin, and J. G. Zhu, "Columnar grain growth of FePt(L10) thin films," *Journal of Applied Physics*, vol. 111, Article ID 07B720, 2012.

[9] Y. Xu, J. S. Chen, and J. P. Wang, "*In situ* ordering of FePt thin films with face-centered-tetragonal (001) texture on $Cr_{100-x}Ru_x$ underlayer at low substrate temperature," *Applied Physics Letters*, vol. 80, no. 18, article 3325, 3 pages, 2002.

[10] Y. C. Wu, L. W. Wang, and C. H. Lai, "Low-temperature ordering of (001) granular FePt films by inserting ultrathin SiO_2 layers," *Applied Physics Letters*, vol. 91, no. 7, Article ID 072502, 3 pages, 2007.

[11] M. L. Yan, N. Powers, and D. J. Sellmyer, "Highly oriented nonepitaxially grown $L1_0$ FePt films," *Journal of Applied Physics*, vol. 93, no. 10, article 8292, 3 pages, 2003.

[12] M. H. Kryder, E. C. Gage, T. W. Mcdaniel et al., "Heat assisted magnetic recording," *Proceedings of the IEEE*, vol. 96, no. 11, pp. 1810–1835, 2008.

[13] D. A. Gilbert, L. W. Wang, T. J. Klemmer, J. U. Thiele, C. H. Lai, and K. Liu, "Tuning magnetic anisotropy in (001) oriented L10 $(Fe_{1-x}Cu_x)_{55}Pt_{45}$ films," *Applied Physics Letters*, vol. 102, no. 13, Article ID 132406, 4 pages, 2013.

[14] J. L. Tsai, H. T. Tzeng, and G. B. Lin, "Magnetization reversal process in Fe/FePt films," *Applied Physics Letters*, vol. 96, no. 3, Article ID 032505, 3 pages, 2010.

[15] R. H. Victora and X. Shen, "Composite media for perpendicular magnetic recording," *IEEE Transactions on Magnetics*, vol. 41, no. 2, pp. 537–542, 2005.

[16] A. Yu. Dobin and H. J. Richter, "Domain wall assisted magnetic recording," *Applied Physics Letters*, vol. 89, no. 6, Article ID 062512, 3 pages, 2006.

[17] D. Goll and A. Breitling, "Coercivity of ledge-type $L1_0$-FePt/Fe nanocomposites with perpendicular magnetization," *Applied Physics Letters*, vol. 94, no. 5, Article ID 052502, 3 pages, 2009.

[18] D. Suess, "Multilayer exchange spring media for magnetic recording," *Applied Physics Letters*, vol. 89, no. 11, Article ID 113105, 3 pages, 2006.

[19] J. L. Tsai, H. T. Tzeng, and B. F. Liu, "Magnetic properties and microstructure of graded Fe/FePt films," *Journal of Applied Physics*, vol. 107, no. 11, Article ID 113923, 5 pages, 2010.

[20] A. Goncharov, T. Schrefl, G. Hrkac et al., "Recording simulations on graded media for area densities of up to 1 Tbit in 2," *Applied Physics Letters*, vol. 91, no. 22, Article ID 222502, 2007.

[21] S. D. Granz and M. H. Kryder, "Granular $L1_0$ FePt (0 0 1) thin films for heat assisted magnetic recording," *Journal of Magnetism and Magnetic Materials*, vol. 324, no. 3, pp. 287–294, 2012.

[22] D. D. Hawn and B. M. Dekoven, "Deconvolution as a correction for photoelectron inelastic energy losses in the core level XPS spectra of iron oxides," *Surface and Interface Analysis*, vol. 10, no. 2-3, pp. 63–74, 1987.

[23] D. Brion, "Etude par spectroscopie de photoelectrons de la degradation superficielle de FeS_2, $CuFeS_2$, ZnS et PbS a l'air et dans l'eau," *Results Applied Surface Science*, vol. 5, no. 2, pp. 133–152, 1980.